THE ASTROPHYSICAL JOURNAL, 297:111–118, 1985 October 1

LEAD, PLATINUM, AND OTHER HEAVY ELEMENTS IN THE PRIMARY COSMIC RADIATION—*HEAO 3* RESULTS

W. R. BINNS,[1] N. R. BREWSTER,[2] D. J. FIXSEN,[2] T. L. GARRARD,[3] M. H. ISRAEL,[1] J. KLARMANN,[1]
B. J. NEWPORT,[3] E. C. STONE,[3] AND C. J. WADDINGTON[2]
Received 1985 February 1; accepted 1985 April 9

ABSTRACT

From an analysis of 580 days of exposure of the Heavy Nuclei Experiment on the *HEAO 3* spacecraft, we have selected 322 nuclei with reasonable charge resolution, $E \geq 1.3$ GeV n^{-1} and $Z \geq 50$. These data show a defined abundance peak in the "platinum" ($74 \leq Z \leq 80$) region, a small abundance of "lead" ($81 \leq Z \leq 83$), and a significant number of "secondary" nuclei in the $62 \leq Z \leq 73$ range. The deduced ratio in space of 0.25 ± 0.09 for "Pb/Pt" is distinctly lower than that predicted by any of the standard models for cosmic-ray sources and propagation effects. Although this low ratio suggests an enrichment in the cosmic-ray source of products of *r*-process nucleosynthesis, it may rather be an indication that the Pb abundance is suppressed by a source fractionation effect, or that there is less Pb in the solar system than is assumed in the standard compilations.

Subject heading: cosmic rays: abundances

I. INTRODUCTION

This paper reports an observation of the abundances of cosmic-ray lead-group and platinum-group nuclei using data from the *HEAO 3* Heavy Nuclei Experiment (HNE). The relative abundances of these elements should provide an indication of the particular mix of nucleosynthesis processes responsible for the creation of these heaviest stable cosmic-ray nuclei. These processes are predominantly neutron captures, which in the extreme proceed via either a rapid, *r*-, or slow, *s*-, chain. The abundance ratio of $_{82}$Pb to the $_{76}$Os, $_{77}$Ir, and $_{78}$Pt group of elements is predicted to be much greater for the *s*-process than for the *r*-process. Hence, a determination of this ratio can provide an important clue to understanding the nature of the sources of the cosmic radiation.

Previously we reported on a search for actinide nuclei (atomic number $Z > 88$) in the cosmic rays using data from *HEAO 3* (Binns *et al.* 1982*a*). In that search we were concerned with the abundance ratio of the actinides to the entire group of elements in the platinum-lead region, and we did not attempt to derive a lead-to-platinum ratio. We concluded from the low observed abundance of actinides that the cosmic rays did not contain a significant contribution of freshly synthesized (less than about 10^7 yr old) *r*-process material, but we could not distinguish between a cosmic-ray source with the same mixture of *r*-process and *s*-process material as in the solar system and one composed only of aged *r*-process material, i.e., *r*-process material like that found in the solar system, over 10^9 yr old, in which all but the longest lived actinides had decayed.

Further analysis of the previously reported data, involving more stringent selections, inclusion of additional data not previously analyzed, and a calibration at the Lawrence Berkeley Laboratory (LBL) Bevalac, have enabled us to obtain the relative abundances of lead and of the platinum group of elements, and hence to determine the abundance ratio. This result, combined with data on the lighter $Z \geq 60$ nuclei, has been used to attempt an interpretation of the significance of these abundances.

The data that we are reporting here have been selected for better charge resolution than in either of our preliminary reports on this subject, presented at Bangalore (Fixsen *et al.* 1983) and COSPAR (Binns *et al.* 1984). All the particles we have included in this paper were required to have had a cutoff rigidity R_c of greater than 5 GV, whereas at Bangalore we also included particles with $R_c < 5$ GV if they had a measured high energy determined from the relative ion chambers and Cherenkov signals. However, those particles with low R_c but high E exhibit a poorer charge resolution than the high-R_c data as characterized by the relevant iron peaks and have been excluded from the present study.

In the COSPAR report, in addition to including particles with $R_c > 5$ GV we also included particles whose energy as measured in the detector was less than 1 GeV n^{-1}. However, these high-charged particles also appeared to have poorer resolution and hence have also been excluded from the present data set.

II. THE DATA SET

The detector (Binns *et al.* 1981) consists of two discrete modules each containing three dual-gap parallel-plate ion chambers with multiwire hodoscopes mounted fore and aft. These modules were mounted on either side of a plastic radiator Cherenkov detector. Particles were accepted if they triggered at least two of the four hodoscopes and at least one of the seven charge measuring devices (six ion chambers and the Cherenkov detector).

In this study we have analyzed 580 days of exposure and considered data for those events where the Cherenkov detector and at least two of the ion chambers were triggered. These data were further refined by selecting only those events which satisfied the following conditions:

1. The trajectory was defined by at least two hodoscopes in which the pattern of wires triggered was not more than eight wires wide in both coordinates, thus eliminating events where interactions or random coincidences resulted in a poorly defined trajectory.

[1] Department of Physics and McDonnell Center for the Space Sciences, Washington University, St. Louis.
[2] School of Physics and Astronomy, University of Minnesota.
[3] George W. Downs Laboratory, California Institute of Technology.

2. Each of the eight phototubes of the Cherenkov detector received at least 4% but not more than 40% of the total Cherenkov signal, eliminating events in which a particle hit a phototube.

3. All the ion chambers that were on the trajectory agreed to within 6%, with those on the same side of the Cherenkov counter agreeing to within 4%, eliminating accidental coincident particles in an ion chamber and some types of interactions.

These data selections are less restrictive than those used in previous publications of HNE data at lower charges, and consequently the charge resolution of these data is not as good; however, the rarity of particles with $Z > 60$ makes these relaxed selections necessary.

Two sets of events satisfying these criteria were then formed—one contains events for which the best estimate of charge was $Z > 49.5$; the other, a "normalization" set, contains 1/400 of all events with $Z > 19.5$, selected at random. This latter set, consisting chiefly of iron and subiron nuclei, allows normalization of the abundances and charges of the heavy elements to that of iron.

III. ANALYSIS

We are reporting here our results based on a sample of those particles which had geomagnetic cut-off rigidities (R) greater than 5 GV ($\approx$1.3 GeV n^{-1}). Nuclei that entered from directions where the cutoff was less than 5 GV have been excluded from our analysis, since the charge assignments that we could make either were ambiguous or resulted in a charge distribution which showed poorer charge resolution than that observed for the higher rigidity events.

The events with $R > 5$ GV were separated into two groups, one with $R > 7$ GV and the other with $5 < R < 7$ GV. The charge scale and resolution for each group were determined independently by examining the iron peak in the corresponding normalization set. In both groups, the nuclear charge of each event was inferred from the Cherenkov signal, assuming that the signal was simply proportional to Z^2. At these rigidities the Cherenkov signal is nearly independent of energy.

A recent calibration of a prototype of the *HEAO* detector with beams of $_{79}$Au with energies up to 1 GeV n^{-1} and $_{25}$Mn with energies up to 1.8 GeV n^{-1} at the LBL Bevalac showed that the ionization signal exhibits appreciable deviations from a Z^2 dependence for high-charge nuclei in an energy range $\lesssim$1.3 GeV n^{-1}, implying corrections that reduce the derived charges by up to 3 charge units (Garrard *et al.* 1983). On the other hand, measurements of the Cherenkov signal at these low energies failed to indicate any clear deviations from a pure Z^2 dependence. Lacking a calibration at the higher energies that are of interest here, we have applied no corrections. If later studies show that such a correction is required, it will presumably be of such a sign as to reduce our assigned charges and specifically reduce our quoted abundance of "lead" relative to "platinum." Monte Carlo modeling of the production of knock-on electrons traversing our detector suggests that it might be necessary to reduce the assumed charge assignments by as much as 1.5 charge units at $Z = 80$ and 0.5 charge units at $Z = 50$ (Derrickson, Eby, and Watts 1984). The effect of such a change will be considered in the following discussion, but essentially only changes the "lead-to-platinum" ratio, reducing it.

Figure 1 shows the observed charge spectrum; 67% of the events have $R > 7$ GV and 33% have $5 < R < 7$ GV. This data set demonstrates an odd-even abundance effect for $50 \leq Z \leq 56$ and a sharp falloff in abundances between 56 and 60, similar to what was found in our previous analysis of a data subset having higher charge resolution (Binns *et al.* 1983). The charge resolution and charge assignments of these data must

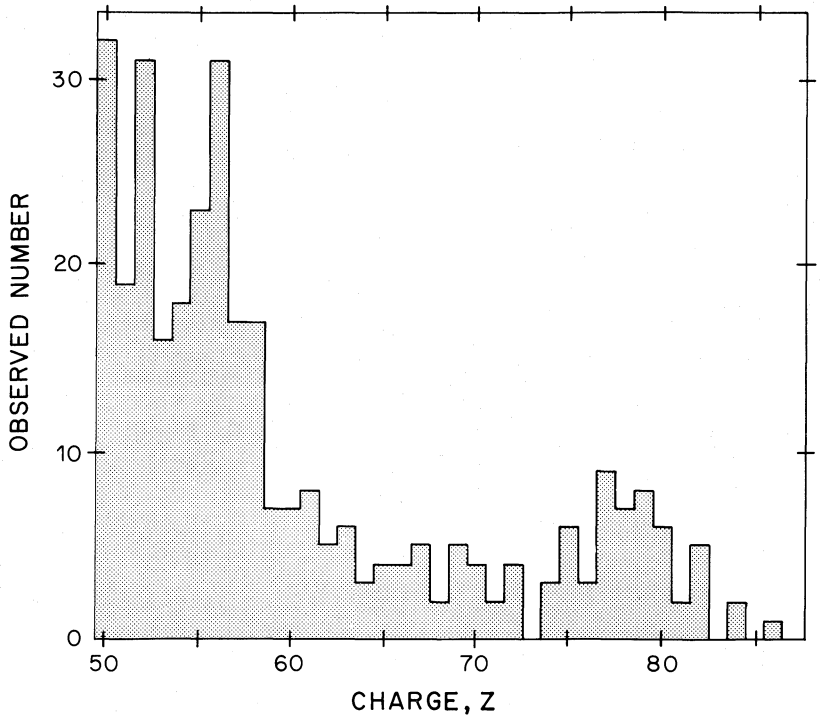

FIG. 1.—Observed charge spectrum with charges assigned assuming a Z^2 dependence of the Cherenkov signal

therefore still be reasonable, even with the relaxed selection criteria used to increase the statistics.

The 322 nuclei with $Z \geq 50$ used in this analysis correspond to $(9.6 \pm 0.5) \times 10^6$ iron nuclei which satisfy the same selection criteria and are observed within the instrument, not in free space. The quoted uncertainty is predominantly due to the uncertainty in resolving $_{25}$Mn from $_{26}$Fe.

Due to the widely varying amounts of matter in the lid and sides of the detector, 1–5 g cm^{-2}, and the thickness of the detector itself, the corrections on individual abundances to free space are considerable, although they are less on abundance ratios. Furthermore, since we have very little experimental or theoretical knowledge of the appropriate nuclear parameters that describe the propagation of ultraheavy (UH) nuclei through media such as aluminum or lucite, these corrections are quite uncertain. One approach to this problem is described in § IV, but any abundance ratios quoted here that are not "in the detector" must be subject to an uncertainty that increases as the range of charges increases.

IV. COMPARISON WITH OTHER DATA

Results that cover this charge range have recently been reported from the *Ariel 6* UH-nuclei detector which was exposed in a 55° inclination orbit (Fowler *et al.* 1984). The reported analysis was for all cutoffs and hence extends to appreciably lower energies than our data. The intrinsic charge resolution of the detector was appreciably less than that of the *HEAO* detector, since at Fe our resolution function from the normalization set is characterized by a FWHM of 0.6 charge units, whereas that for *Ariel* appears to have been at least twice as large. In order to analyze the *Ariel* data, Fowler *et al.* had therefore to deconvolve their data using an extrapolation of the resolution function found for Fe and lighter nuclei.

We have chosen not to attempt a deconvolution of our charge spectrum, since the results of such a process are quite sensitive to the form of the assumed resolution function, particularly when individual element peaks are not apparent in the data. Any comparison between our results and those reported from Ariel should take this into account. Due to the limited charge resolution in the data we have considered only the following physically significant groups of charges, listed with the number of nuclei observed:[4]

"Lead," $N(81 \leq Z \leq 86)$	10
"Platinum," $N(74 \leq Z \leq 80)$	42
"Heavy secondary" (HS), $N(70 \leq Z \leq 73)$	10
"Light secondary" (LS), $N(62 \leq Z \leq 69)$	34
"Tin," $N(50 \leq Z \leq 58)$	204

[4] It should be noted that these groups differ slightly from those used previously, e.g., Fixsen *et al.* (1983).

We have chosen to include the observed events with charge 80 in the Pt rather than the Pb group for two reasons. First, taking account of the instrument resolution and the observed numbers of events with $Z < 80$ and $Z > 80$, it is more likely that the observed events assigned $Z = 80$ are smeared by resolution from the Pt group. Second, suggested correction models for deviation of the Cherenkov response from Z^2 would decrease assigned charges down about one charge unit, in which case the observed events which had been assigned $Z = 80$ would certainly belong to the Pt group.

Ratios of the abundances in these groups will be compared with other data and with model predictions. Our discussion will mainly be in terms of the ratios: lead to platinum, heavy secondaries to lead plus platinum, light secondaries to lead plus platinum, and lead plus platinum to tin.

The values derived from our observations of these ratios differ from the true values outside the detector because of two effects. First, particles undergo nuclear interactions as they enter and penetrate the instrument. Second, the instrumental resolution, characterized by a standard deviation of approximately one charge unit at Pt, smears the charge distribution. We have derived a correction factor for each of the four ratios to correct for both these effects. For each of eight plausible models, we calculated abundances expected near Earth, as described below in § V. Entry into the detector was then simulated by propagation through various slabs of hydrogen approximating the amount of aluminum in the various paths into and through the detector. (Using hydrogen cross sections introduces an unknown bias into the model, but true cross sections for these nuclei on aluminum, the major component of the detector, are unknown at present. However, errors in the cross sections for any one element are likely to be largely duplicated in the other elements, making abundance ratios relatively insensitive.) The resulting element distribution inside the detector was then convolved with the instrument resolution to derive the distribution we would expect to observe. Although the eight models gave very different values for the ratios of interest at the outside of the instrument, the factor by which these ratios changed after propagation into the instrument and convolution with the resolution was nearly the same for all the models. Therefore, we have used a single correction factor for each of the ratios.

In Table 1, column (2) shows the observed abundance ratios and column (3) the correction factors. The product of these two columns, shown in column (4), gives our results outside the detector. Column (5) gives the corresponding result reported by the *Ariel* experiment, while column (6) gives the ratio of our *HEAO* results to those of *Ariel*. Although there is good agreement between our results and those of *Ariel* for the ratio of the two dominant groups of primary elements, PbPt/Sn, for each of the other three ratios our result is about 60%–65% of

TABLE 1

	HEAO Results			*Ariel* Outside Detector	*HEAO/Ariel* Outside Detector
Ratio (1)	Inside Detector (2)	Correction Factor (3)	Outside Detector (4)	(5)	(6)
Pb/Pt	0.24 ± 0.08	1.06 ± 0.02	0.25 ± 0.09	0.40 ± 0.10	0.63 ± 0.26
HS/PbPt	0.19 ± 0.07	0.85 ± 0.02	0.16 ± 0.06	0.27 ± 0.07	0.59 ± 0.27
LS/PbPt	0.65 ± 0.14	0.87 ± 0.02	0.57 ± 0.12	0.88 ± 0.15	0.65 ± 0.18
PbPt/Sn	0.25 ± 0.04	1.10 ± 0.03	0.28 ± 0.05	0.29 ± 0.04	0.97 ± 0.22

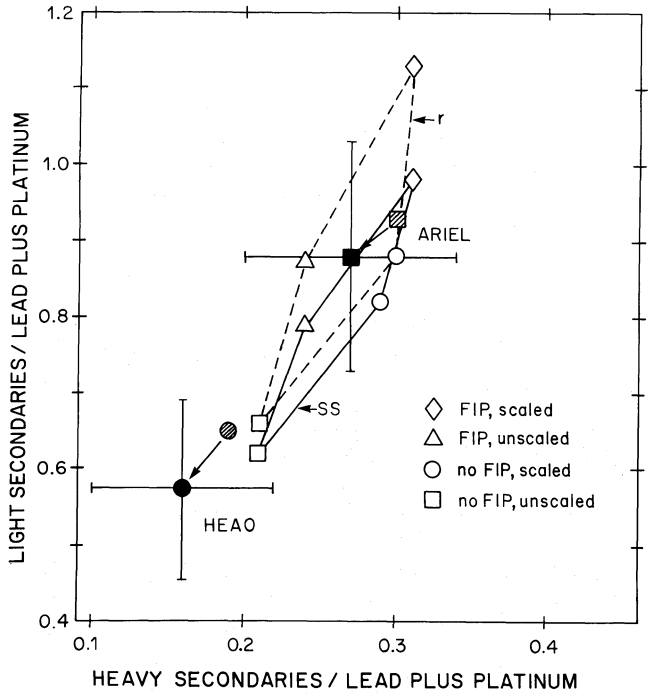

FIG. 2.—Comparison of the observed and predicted abundance ratios "light secondaries"/PbPt and "heavy secondaries"/PbPt. Observed values are shaded, and those outside the detector are solid with error bars. Predicted values are for solar system or *r*-process sources with four different assumptions. Note that the *HEAO* data are limited to $R_c > 5$ GV, while the *Ariel* data include particles with $R \gtrsim 1$ GV. The calculated values are for the same mix of rigidities as the *HEAO* data.

Ariel's. While these differences are only significant at a level of 1.5–2.0 standard deviations, it is unlikely that they are all just statistical fluctuations. We believe that these differences may reflect a broad spillover to higher apparent charges in the *Ariel* data which is not adequately accounted for in their deconvolution. Such an effect also appears to have occurred in our own earlier analysis, Binns *et al.* (1984), because of the inclusion of poor-resolution data of lower energy, which we have now omitted. An alternative explanation could be that the secondary abundance ratios are energy-dependent.

V. COMPARISON WITH MODELS

Our observed charge spectrum, Figure 1, or the abundance ratios constructed from it, can be compared with what would be predicted by various models. A series of predictions were made using the solar system abundances of Anders and Ebihara (1982), the *s*-process contribution to these abundances calculated using neutron-capture cross sections and an *s*-process model, and the *r*-process contribution derived by subtracting the *s*-process abundances from the solar system total (see Appendix). These various abundances, taken as calculated, or adjusted for a model of first ionization potential (FIP) fractionation (Brewster, Freier, and Waddington 1983), were used as source abundances. These were then propagated through the interstellar medium, assuming a leaky-box model, and using the revised code of Brewster, Freier, and Waddington (1985) with a rigidity-dependent escape length (Ormes and Protheroe 1983) that is 6.21 g cm^{-2} of hydrogen at 7 GV. The partial nuclear interaction cross sections of these heavy elements on hydrogen are not well determined. Consequently we have used both the cross sections calculated from the formalism of Silberberg and Tsao (1973*a*, *b*) and these cross sections scaled to agree with recent measurements of the fragmentation of a 1 GeV n^{-1} $_{79}$Au beam at the LBL Bevalac (Brewster *et al.* 1983). The predictions of this program, which, with the inclusion of additional isotopes for each element led to significantly increased ratios of secondary-to-primary charge groups, are in good agreement with the latest predictions obtained by Margolis and Blake (1983), at least for the solar system source abundances.

In Figures 2 and 3, we show calculated values of these ratios for solar system abundances and for *r*-process abundances; *s*-process abundances are not given because they show little relation to the observed values, with lead-to-platinum ratios of ~ 1.0. In each case we give the values with and without an adjustment for FIP and with and without a correction on the cross sections for scaling.

VI. DISCUSSION

We first examine the results for the abundances of the secondary nuclei, $62 \leq Z \leq 73$, relative to the nuclei of the platinum-plus-lead group. These suggest the adoption of one of the propagation models discussed above. Then we examine the results for the lead-to-platinum ratio in this context.

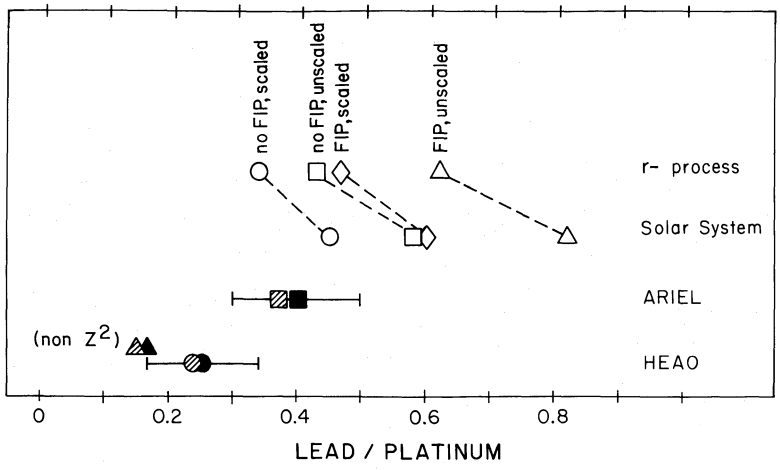

FIG. 3.—The "lead-to-platinum" ratio as observed and predicted. Observed values are shown shaded, while values outside the detector are shown solid and with error bars. The shaded and solid triangles indicate the ratios when a non-Z^2 correction to our charge assignments is included.

a) Secondary Ratios

Our observed values of the secondary ratios (Fig. 2) are in reasonable agreement with the prediction based on a model without FIP fractionation at the source and without scaling of the cross sections; however, our observations are in distinct disagreement with the models that include FIP fractionation or scaling of cross sections. These secondary ratios do not distinguish between solar-system and *r*-process abundances at the source, since, with the exception of lead, not only are solar system abundances of most of the elements with $Z > 60$ dominated by the *r*-process contributions, but the secondary production is largely independent of the precise composition of the primaries.

The scaled cross sections were introduced in an attempt to account for the measured discrepancies between the observed and calculated values of the fragmentation cross sections of gold nuclei. The differences between the results with scaled and those with unscaled cross sections is a measure of the effect of the uncertainties in the cross sections. The fact that scaling the cross sections makes the agreement worse may indicate that results obtained for one odd-charged projectile, $_{79}$Au, do not adequately describe the interaction characteristics of the majority of the nuclides in the lead to platinum group.

Similarly, the best apparent fit is with a prediction that does not adjust the source abundances for FIP fractionation, which is contrary to the conclusions found at lower charges (Binns *et al.* 1982*b*, 1983), where observed abundances agreed better with those expected from a solar system source with FIP fractionation than without it. However, this could be explained if the form of the fit to the FIP dependence is not a simple exponential, as used in the predictions plotted here, but instead has a step function form of the kind suggested by Cook *et al.* (1979) and Meyer (1981) with a step that introduces a correction only for elements with a potential greater than about 9 eV, so that lead, platinum, and most of the secondaries would be unaffected.

b) Lead and Platinum

Our observed ratio for Pb/Pt (Fig. 3) is distinctly lower than that predicted from solar system source abundances in any of the four models considered. In particular, using the model in best agreement with the secondary results, without scaling cross sections and without FIP fractionation, the observed ratio is distinctly lower than predicted from either a solar system or an *r*-process source. This result might suggest that, unlike the cosmic rays with $Z < 60$ (Binns *et al.* 1982*b*, 1983), the cosmic rays with $Z \approx 80$ come from a source with a distinctly different nucleosynthesis history from that of the solar system elements. However, two alternatives to this conclusion must also be considered. First, the Pb abundance in the cosmic-ray source may be suppressed by some form of source fractionation which depends on a different parameter than FIP. Second, it could be that the Pb abundances assumed in our model calculations are not really representative of the solar system or of the *r*- or *s*-process contributions to the solar system.

We have noted (Israel *et al.* 1983) that the cosmic-ray abundance of Ge relative to Fe is down by a factor of ~ 2 compared to the solar system. Ge, like Pb, is one of the few volatile elements with moderate-to-low FIP. The factor-of-two underabundance of Ge lends support to the suggestion (Cesarsky and Bibring 1980; Epstein 1980) that it is volatile elements, rather than elements with high FIP, which are underabundant in the cosmic rays. Such a source fractionation dependent on volatility could produce our observed low Pb abundance even with a cosmic-ray source whose composition is essentially the same as that of the solar system.

Alternatively, there are reasons for believing that the source abundances of Pb used in our models may not be representative of the solar system values. The *r*-process Pb abundance we used was derived by Fixsen (1985) by subtracting an *s*-process component from the Anders and Ebihara solar system abundances. However, Fixsen has argued that interpolation between *r*-process isotopes of $_{81}$Tl and $_{83}$Bi strongly suggests a lower *r*-process abundance of $_{82}$Pb than indicated here. Similarly, Cameron's decomposition (1982*a*) of his solar system abundances gave an *r*-process with much less Pb than we used in our model. Our observed Pb/Pt ratio could be consistent with that expected from such a "Pb-poor *r*-process," either with or without FIP fractionation.

Furthermore, if the *r*-process Pb abundance obtained by subtracting the *s*-process contribution from the assumed solar system value is too high, then it is possible that the assumed solar system Pb abundance itself is too high. If the Anders and Ebihara Pb abundance were twice that of typical solar system matter, then a solar system source abundance, either with or without FIP fractionation, would agree with our data.

Finally, we note that Ge and Pb, like most elements with higher FIP, have abundances in C2 chondritic meteorites about a factor of 2 lower than abundances in the C1 chondrites which are the basis for the Anders and Ebihara solar system abundances. If the C2 rather than the C1 chondrites were more nearly representative of the composition of the heavier elements in the solar system, then our low Pb/Pt ratio would again be consistent with a cosmic-ray source of composition similar to that of the solar system.

Thus, while our Pb/Pt ratio is distinctly lower than that predicted by any of the standard models for cosmic-ray sources, it is possible that the difference is not an indication that the cosmic-ray source composition is greatly different from that of the solar system, but rather that there is less Pb in the solar system and in the *r*-process than is assumed in the standard model.

We thank L. Atchison for assistance in programming for data analysis. The research was supported in part by NASA under contracts NAS 8-27976, 77, 78, and grants NGR 05-002-160, 24-005-050, and 26-008-001.

APPENDIX

DECONVOLUTION OF SOLAR SYSTEM ABUNDANCES

The Anders and Ebihara (1982) solar composition data have been combined with recently published neutron capture cross sections, Kappeler *et al.* (1982), and with the assumption of a single exponential neutron flux distribution to estimate the contribution of the *s*-process to the observed abundances. The method of deconvolution used to deduce the *r*-process abundances from these

TABLE 2

ABUNDANCES RELATIVE TO Si = 10^6

Z	A	Solar Abundance[a]	Cross Section (mbarn)	s-Process	r-Process
34[b]	80	32000	90 ± 60%	2400 ± 1400	30000 ± 3500
35	81	5800	480 ± 17%	450 ± 76	5400 ± 1700
36	82	11000	110 ± 14%	2000 ± 280	8900 ± 1600
36	83	5200	270 ± 10%	750 ± 75	400 ± 730
36[b]	84	26000	39 ± 8%	4800 ± 380	21000 ± 3600
37	85	5100	220 ± 9%	860 ± 77	4300 ± 820
38	86	2300	74 ± 9%	2300 ± 210	...
36	86	7900	...	...	7900 ± 1100
38	87	1600	91 ± 8%	1600 ± 150	...
37	87	2100	...	...	2100 ± 290
38	88	20000	6 ± 17%	18000 ± 3100	1600 ± 3500
39	89	4600	21 ± 15%	4500 ± 680	130 ± 790
40	90	5500	15 ± 21%	5100 ± 1100	360 ± 1500
40	91	1200	64 ± 12%	1100 ± 130	93 ± 250
40	92	1800	43 ± 23%	1500 ± 350	300 ± 480
41[c]	93	710	81 ± 6%	780 ± 47	−67 ± 220
40	94	1900	27 ± 10%	2100 ± 210	−210 ± 390
42	95	400	430 ± 12%	130 ± 16	270 ± 190
42	96	420	110 ± 12%	420 ± 200	...
40	96	300	...	...	300 ± 54
42	97	240	350 ± 14%	150 ± 21	90 ± 120
42	98	610	130 ± 27%	410 ± 110	200 ± 310
44[c]	99	240	640 ± 9%	80 ± 7.2	160 ± 16
44	100	230	210 ± 5%	230 ± 14	...
42	100	240	...	...	240 ± 110
44	101	320	1000 ± 3%	50 ± 1.5	270 ± 19
44	102	590	190 ± 3%	260 ± 7.9	330 ± 36
45	103	340	1100 ± 3%	46 ± 1.4	300 ± 62
46	104	150	450 ± 5%	150 ± 15	...
44	104	350	...	...	350 ± 21
46	105	310	1200 ± 5%	41 ± 2.1	270 ± 31
46	106	380	380 ± 5%	130 ± 6.3	250 ± 38
47[c]	107	270	950 ± 11%	51 ± 5.6	220 ± 44
46	108	370	350 ± 5%	140 ± 6.9	230 ± 38
47	109	260	620 ± 8%	77 ± 6.1	180 ± 41
48	110	200	260 ± 12%	200 ± 14	...
46	110	160	...	...	160 ± 16
48	111	200	620 ± 10%	75 ± 7.5	130 ± 16
48	112	380	230 ± 13%	200 ± 26	190 ± 37
48	113	190	570 ± 9%	80 ± 7.2	110 ± 15
48	114	460	160 ± 16%	280 ± 45	170 ± 55
49	115	190	750 ± 6%	59 ± 3.6	130 ± 14
50	116	570	97 ± 20%	570 ± 57	...
48	116	120	...	...	120 ± 8.3
50	117	300	420 ± 7%	100 ± 7.1	190 ± 30
50	118	930	63 ± 8%	640 ± 51	290 ± 110
50	119	330	260 ± 16%	150 ± 25	180 ± 41
50	120	1200	50 ± 30%	750 ± 220	490 ± 260
51	121	200	840 ± 14%	44 ± 6.2	160 ± 45
52	122	120	310 ± 20%	120 ± 38	...
50	122	170	...	...	170 ± 17
52	123	44	910 ± 10%	44 ± 9.7	...
51	123	150	...	...	150 ± 11
52	124	230	170 ± 12%	230 ± 70	...
50	124	220	...	...	220 ± 22
52	125	340	430 ± 5%	83 ± 4.1	260 ± 110
52	126	920	71 ± 10%	480 ± 48	440 ± 290
53	127	900	760 ± 5%	45 ± 2.2	860 ± 360
54	128	94	300 ± 50%	94 ± 30	...
52	128	1600	...	...	1600 ± 480
54	129	1200	540 ± 8%	62 ± 4.9	1100 ± 380
54	130	190	180 ± 28%	190 ± 61	...
52	130	1700	...	...	1700 ± 520
54	131	940	510 ± 9%	64 ± 5.7	880 ± 300
54	132	1200	120 ± 5%	260 ± 13	890 ± 370
55	133	370	710 ± 6%	44 ± 2.7	330 ± 30
56	134	110	230 ± 16%	110 ± 12	...
54	134	420	...	...	420 ± 130
56	135	290	470 ± 11%	65 ± 7.2	220 ± 32
56	136	320	70 ± 14%	320 ± 36	...

TABLE 2—*Continued*

Z	A	Solar Abundance[a]	Cross Section (mbarn)	*s*-Process	*r*-Process
54.....	136	340	...	...	340 ± 110
56.....	137	490	58 ± 7%	480 ± 33	13 ± 63
56.....	138	3100	4.2 ± 6%	3600 ± 220	−470 ± 410
57.....	139	490	40 ± 15%	350 ± 52	140 ± 100
58.....	140	1000	12 ± 5%	940 ± 47	90 ± 110
59.....	141	170	110 ± 11%	94 ± 10	80 ± 20
60.....	142	230	49 ± 8%	230 ± 23	...
58.....	142	130	...	...	130 ± 13
60.....	143	100	260 ± 4%	37 ± 3.3	65 ± 11
60.....	144	200	120 ± 5%	140 ± 14	58 ± 24
60.....	145	69	510 ± 22%	20 ± 2.0	49 ± 7.2
60.....	146	140	130 ± 16%	77 ± 7.7	67 ± 16
62.....	147	41	1200 ± 8%	7.7 ± 0.6	33 ± 4.1
62.....	148	30	280 ± 8%	30 ± 3.0	...
60.....	148	48	...	...	48 ± 4.8
62.....	149	36	2600 ± 17%	3.3 ± 0.6	33 ± 3.6
62.....	150	19	580 ± 33%	19 ± 1.9	...
60.....	150	47	...	...	47 ± 4.7
63.....	151	47	4600 ± 25%	1.9 ± 0.5	45 ± 4.7
62[c].....	152	69	430 ± 11%	20 ± 2.2	48 ± 7.2
63.....	153	51	2700 ± 11%	3.2 ± 0.3	48 ± 5.1
64.....	154	7.0	1300 ± 9%	7.0 ± 2.1	...
62.....	154	59	...	...	59 ± 5.9
64.....	155	49	2700 ± 10%	3.1 ± 0.3	46 ± 15
64.....	156	68	560 ± 10%	15 ± 1.5	53 ± 21
64.....	157	52	1500 ± 10%	5.8 ± 0.6	46 ± 16
64.....	158	82	430 ± 13%	20 ± 2.6	62 ± 25
65.....	159	59	2000 ± 12%	4.1 ± 0.5	55 ± 18
66.....	160	9.0	800 ± 33%	9.0 ± 0.9	...
64.....	160	72	...	...	72 ± 22
66.....	161	76	2800 ± 11%	3.0 ± 0.3	73 ± 7.6
66.....	162	100	470 ± 11%	18 ± 1.9	83 ± 10
66.....	163	99	1600 ± 19%	5.2 ± 1.0	94 ± 9.9
66.....	164	110	180 ± 22%	45 ± 9.9	69 ± 15
67.....	165	88	1300 ± 5%	6.4 ± 0.3	82 ± 8.8
68.....	166	85	520 ± 8%	16 ± 1.2	70 ± 8.6
68.....	167	58	1400 ± 11%	5.6 ± 0.6	52 ± 5.8
68.....	168	69	240 ± 9%	33 ± 2.9	37 ± 7.5
69.....	169	37	1100 ± 14%	7.0 ± 1.0	30 ± 3.8
70.....	170	7.5	770 ± 4%	7.5 ± 1.0	30 ± 3.8
68.....	170	38	...	...	38 ± 3.8
70.....	171	35	1500 ± 10%	5.4 ± 0.5	30 ± 7.0
70.....	172	53	410 ± 9%	19 ± 1.7	34 ± 11
70.....	173	39	870 ± 8%	8.9 ± 0.7	30 ± 7.8
70.....	174	77	180 ± 14%	43 ± 6.1	34 ± 17
71.....	175	36	1300 ± 8%	6.0 ± 0.5	30 ± 3.6
72[d].....	176	10	1100 ± 25%	10 ± 0.8	...
70.....	176	31	...	...	31 ± 6.2
72.....	177	33	1500 ± 10%	5.0 ± 0.5	28 ± 2.7
72.....	178	48	330 ± 12%	23 ± 2.7	26 ± 4.7
72.....	179	24	1400 ± 12%	5.5 ± 0.7	19 ± 2.0
72.....	180	62	180 ± 28%	42 ± 12	21 ± 13
73.....	181	23	800 ± 10%	9.0 ± 0.9	14 ± 3.6
74.....	182	36	320 ± 12%	22 ± 2.7	14 ± 29
74.....	183	20	550 ± 9%	13 ± 1.2	7.1 ± 16
74.....	184	42	270 ± 11%	27 ± 2.9	16 ± 34
75.....	185	19	1500 ± 13%	4.6 ± 0.6	14 ± 2.4
76.....	186	12	470 ± 4%	12 ± 1.1	...
74.....	186	39	...	...	39 ± 31
76.....	187	9.0	920 ± 2%	9.0 ± 0.9	...
75.....	187	34	...	...	34 ± 27
76.....	188	95	400 ± 4%	17 ± 0.7	78 ± 9.5
76.....	189	120	1500 ± 10%	4.5 ± 0.4	110 ± 12
76.....	190	190	300 ± 10%	23 ± 2.3	170 ± 19
77.....	191	250	1300 ± 16%	5.1 ± 0.8	240 ± 27
78.....	192	11	460 ± 52%	11 ± 1.1	...
76.....	192	290	...	...	290 ± 29
77.....	193	410	800 ± 13%	8.4 ± 1.1	410 ± 46
78.....	194	450	390 ± 10%	17 ± 1.7	430 ± 45
78.....	195	460	1000 ± 10%	6.3 ± 0.6	460 ± 46
78.....	196	350	160 ± 25%	40 ± 10	310 ± 36
79.....	197	190	610 ± 2%	11 ± 0.2	180 ± 37

TABLE 2—*Continued*

Z	A	Solar Abundance[a]	Cross Section (mbarn)	*s*-Process	*r*-Process
80.....	198	52	460 ± 50%	52 ± 41	...
78.....	198	99	...	...	99 ± 9.9
80.....	199	87	360 ± 11%	18 ± 1.9	70 ± 69
80.....	200	120	69 ± 7%	87 ± 6.1	33 ± 95
80.....	201	69	130 ± 9%	45 ± 4.1	24 ± 55
80.....	202	160	45 ± 30%	120 ± 36	34 ± 130
81.....	203	54	150 ± 9%	36 ± 3.2	19 ± 6.3
82.....	204	61	59 ± 18%	61 ± 13	...
80.....	204	36	...	...	36 ± 28
81[c].....	205	130	58 ± 10%	83 ± 8.3	47 ± 15
82.....	206	590	15 ± 7%	280 ± 19	310 ± 130
82.....	207	640	11 ± 9%	310 ± 25	350 ± 140
82.....	208	1800	0.61 ± 25%	780 ± 180	1000 ± 420
83.....	209	140	11 ± 18%	33 ± 5.5	120 ± 14
90.....	232	42	...	...	42 ± 15
92.....	235	5.7	...	...	5.7 ± 3.1
92.....	238	18	...	...	18 ± 10

NOTE.—Solar system data are for 4.6×10^9 yr ago.
[a] From Anders and Ebihara 1982.
[b] Helium burning process is significant, and therefore the *r*-process estimation is too high.
[c] Decay products of the original *s*-process, and the cross section given is for the parent nuclide.
[d] Major path of *s*-process.

data closely followed those used earlier by Seeger, Fowler, and Clayton (1965) and Kappeler *et al.* (1982) on previous compilation of solar system abundances. A detailed discussion is given in a report by Fixsen (1985).

Table 2 shows the solar abundances, the 30 keV neutron cross sections in mbarn with their assigned errors, and the *s*- and *r*-process abundances with estimated uncertainties. These abundances may be compared with those deconvolved previously by Israel *et al.* (1981) and Cameron (1982*a*), which were based on the earlier solar abundance compilation of Cameron (1982*b*). These deconvolutions principally differ in their treatment of the lead abundances and the use of different solar abundances.

REFERENCES

Anders, E., and Ebihara, M. 1982, *Geochim. et Cosmochim.*, **46**, 2363.
Binns, W. R., Fickle, R. K., Garrard, T. L., Israel, M. H., Klarmann, J., Krombel, K. E., Stone, E. C., and Waddington, C. J. 1983, *Ap. J. (Letters)*, **267**, L93.
Binns, W. R., Fickle, R. K., Garrard, T. L., Israel, M. H., Klarmann, J., Stone, E. C., and Waddington, C. J. 1982*a*, *Ap. J. (Letters)*, **261**, L117.
———. 1982*b*, *Ap. J. (Letters)*, **247**, L115.
Binns, W. R., Fixsen, D. J., Garrard, T. L., Israel, M. H., Klarmann, J., Stone, E. C., and Waddington, C. J. 1984, *Adv. Space Res.*, **4**, 25.
Binns, W. R., Israel, M. H., Klarmann, J., Scarlett, W. R., Stone, E. C., and Waddington, C. J. 1981, *Nucl. Instr. Methods*, **185**, 415.
Brewster, N. R., *et al.* 1983, *18th International Cosmic Ray Conference* (Bangalore), Vol. **9**, p. 259.
Brewster, N. R., Freier, P. S., and Waddington, C. J. 1983, *Ap. J.*, **264**, 324.
———. 1985, *Ap. J.*, **294**, 419.
Cameron, A. G. W. 1982*a*, *Ap. Space Sci.*, **82**, 123.
———. 1982*b*, in *Essays in Nuclear Astrophysics*, ed. C. A. Barnes, D. D. Clayton, and D. N. Schramm (Cambridge: Cambridge University Press), p. 23.
Cesarsky, C. J., and Bibring, J. P. 1980, *IAU Symposium 94, Origin of Cosmic Rays*, ed. G. Setti, G. Spada, and A. W. Wolfendale (Dordrecht: Reidel), p. 361.
Cook, W. R., Stone, E. C., Vogt, R. E., Trainor, J. H., and Webber, W. R. 1979, *16th International Cosmic Ray Conference* (Kyoto), Vol. **12**, p. 265.
Derrickson, J. H., Eby, P. B., and Watts, J. W. 1984, *Nucl. Instr. Methods*, **225**, 185.
Epstein, R. I. 1980, *M.N.R.A.S.*, **193**, 723.
Fixsen, D. J. 1985, University of Minnesota Cosmic Ray Report, No. CR-195.
Fixsen, D. J., Waddington, C. J., Binns, W. R., Israel, M. H., Klarmann, J., Garrard, T. L., Newport, B. J., and Stone, E. C. 1983, *18th International Cosmic Ray Conference* (Bangalore), Vol. **9**, p. 119.
Fowler, P. H., Masheder, M. R. W., Moses, R. T., Walker, R. N. F., and Worley, A. 1984, unpublished paper presented at ninth European Cosmic Ray Symposium.
Garrard, T. L., *et al.* 1983, *18th International Cosmic Ray Conference* (Bangalore), Vol. **9**, p. 367.
Israel, M. H., *et al.* 1983, *18th International Cosmic Ray Conference* (Bangalore), Vol. **9**, p. 305.
Israel, M. H., Klarmann, J., Binns, W. R., Fickle, R. K., Waddington, C. J., Garrard, T. L., and Stone, E. C. 1981, *17th International Cosmic Ray Conference* (Paris), Vol. **2**, p. 36.
Kappeler, F., Beer, H., Wisshak, T., Clayton, D. D., Macklin, R. L., and Ward, R. A. 1982, *Ap. J.*, **257**, 821.
Margolis, S. H., and Blake, J. B. 1983, *18th International Cosmic Ray Conference* (Bangalore), Vol. **9**, p. 283.
Meyer, J. P. 1981, *17th International Cosmic Ray Conference* (Paris), Vol. **2**, p. 281.
Ormes, J. F., and Protheroe, R. J. 1983, *Ap. J.*, **272**, 756.
Seeger, P. A., Fowler, W. A., and Clayton, D. D. 1965, *Ap. J. Suppl.*, **11**, 121.
Silberberg, R., and Tsao, C. H. 1973*a*, *Ap. J. Suppl.*, **25**, 315.
———. 1973*b*, *Ap. J. Suppl.*, **25**, 335.

W. R. BINNS, M. H. ISRAEL, and J. KLARMANN: Department of Physics and the McDonnell Center for the Space Sciences, Washington University, St. Louis, MO 63130

N. R. BREWSTER, D. J. FIXSEN, and C. J. WADDINGTON: School of Physics and Astronomy, University of Minnesota, 116 Church St. S.E., Minneapolis, MN 55455

T. L. GARRARD, B. J. NEWPORT, and E. C. STONE: 220-47 Downs Laboratory, California Institute of Technology, Pasadena, CA 91125